HHS Public Access

Author manuscript

J Am Chem Soc. Author manuscript; available in PMC 2020 April 10.

Published in final edited form as:

J Am Chem Soc. 2019 April 10; 141(14): 5659–5663. doi:10.1021/jacs.9b02204.

Enzyme-catalyzed inverse-electron demand Diels-Alder reaction in the biosynthesis of antifungal ilicicolin H

Zhuan Zhang[1], **Cooper S. Jamieson**[2], **Yi-Lei Zhao**[2,3], **Dehai Li**[4], **Masao Ohashi**[1], **K. N. Houk**[1,2], and **Yi Tang**[1,2]

[1]Department of Chemical and Biomolecular Engineering, University of California, Los Angeles, California 90095, USA

[2]Department of Chemistry and Biochemistry, University of California, Los Angeles, California 90095, USA

[3]State Key Laboratory of Microbial Metabolism, Joint International Research Laboratory of Metabolic and Developmental Sciences, MOE-LSB and MOE-LSC, School of Life Sciences and Biotechnology, Shanghai Jiao Tong University, Shanghai 200240, China

[4]Key Laboratory of Marine Drugs, Chinese Ministry of Education, School of Medicine and Pharmacy, Laboratory for Marine Drugs and Bioproducts, Pilot National Laboratory for Marine Science and Technology, Ocean University of China, Qingdao 266003, China

Abstract

The pericyclases are a growing superfamily of enzymes that catalyze pericyclic reactions. We report a pericyclase IccD catalyzing an inverse-electron demand Diels–Alder (IEDDA) reaction with a rate acceleration of 3×10^5 fold in the biosynthesis of fungal natural product ilicicolin H. We demonstrate IccD is highly periselective towards the IEDDA cycloaddition over a competing normal electron demand Diels-Alder (NEDDA) reaction from an ambimodal transition state. A predicted flavoenzyme IccE was identified to epimerize the IEDDA product 8-*epi*-ilicicolin H to ilicicolin H, a step that is critical for the observed antifungal activity of ilicicolin H. Our results reveal the ilicicolin H biosynthetic pathway and add to the collection of pericyclic reactions that are catalyzed by pericyclases.

Graphical Abstract

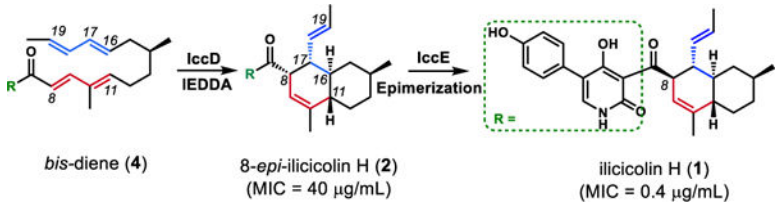

Corresponding Author Yi Tang yitang@ucla.edu; K. N. Houk houk@chem.ucla.edu; Masao Ohashi gph422001@ucla.edu.

ASSOCIATED CONTENT

Supporting Information

Experimental details, spectroscopic and computational data. This material is available free of charge via the Internet at http://pubs.acs.org.

Diels-Alder (DA) reactions, involving the cycloaddition between a 1,3-diene and a dienophile to form an unsaturated six-membered ring, are among the most powerful synthetic transformations to construct complex natural products.[1] Depending on substituents, the reaction can proceed via the normal- or inverse-electron demand Diels-Alder (NEDDA or IEDDA) pathways that differ in relative frontier molecular orbital (FMO, HOMO–LUMO) energies (Figure 1A). Hundreds of natural products with unsaturated cyclohexenes or octahydrodecalins have been identified. [2] Many of these are products of pericyclic reactions, and it is now known that a variety of pericyclases—enzymes that catalyze pericyclic reactions—exist.[3] PyrE3,[4] CghA[5] and MycB,[6] and others,[7,8] are all decalin-forming pericyclases that catalyze NEDDA reactions (Figure 1A). In contrast, no enzyme-catalyzed IEDDA reaction has been reported to date. Structural examination and biomimetic synthesis of natural products, however, suggest enzyme-catalyzed IEDDA reaction should exist in Nature.[9]

One potential IEDDA pericyclase candidate is in the biosynthetic pathway of ilicicolin H (**1**) (Figure 1B).[10] The decalin-containing **1** was isolated from *Cylindrocladium ilicicola* MFC-870 and other fungi. [10,11] **1** is a 4-hydroxy-2-pyridone alkaloid, and has a potent (sub μg/mL) and broad (*Candida*, *Aspergillus* and *Cryptococcus*) antifungal activities by inhibiting the mitochondrial respiration chain.[12] While the biosynthesis of **1** has remained unresolved, a biomimetic total synthesis of (±)-**1** was reported by Williams *et al.* using an intramolecular IEDDA step to form the *trans*-octahydrodecalin.[13] A model study using an ethyl ester of the acyclic precursor showed that heating the *bis*-diene compound in boiling water or refluxing toluene afforded opposite selectivity towards IEDDA or NEDDA reaction (Figure 1B).[14] Pericyclic reaction selectivity can be rationalized by FMOs, and selectivity for a specific pericyclic reaction is referred to as periselectivity.[15] The synthetic results therefore indicated that NEDDA and IEDDA reactions are competitive, and periselectivity depends on solvent polarity (Figure 1B). The synthetic studies were not able to afford only the desired IEDDA product. This led us to hypothesize that an enzyme must control the IEDDA periselectivity in biosynthesis of **1**.

To identify the responsible enzyme, we first searched for candidate genes that are likely to participate in the biosynthesis of **1** in the genome sequence of a producing fungus, *Nectria* sp. B-13.[11b] As with other fungal 2-pyridone compounds, we propose biosynthesis of **1** starts with formation of the tetramic acid **3** by a polyketide non-ribosomal peptide synthetase (PKS-NRPS) with a partnering enoylreductase (ER), followed by a P450-catalyzed ring expansion of the tetramate to the acyclic **4**.[16] This led to the identification of one candidate cluster *ncc* that contains five genes, encoding a PKS-NRPS (*nccA*), a partnering ER (*nccB*), a P450 (*nccC*), a predicted *C*-methyltransferase (*C*-MT, *nccD*), and a predicted old yellow enzyme (OYE, *nccE*) (Figure 2A, Table S3). We searched for homologs of this five-gene cassette computationally, which revealed this combination is widely distributed in fungi: 41 different sequenced fungal strains in the NCBI database were found to minimally contain the five-gene pathway (Figure S1). For example, we identified the *icc* cluster that contains the five genes from the recently sequenced *Penicillium variabile* (Figure 2A, Table S3).[17] The cDNA library of *P. variable* was available to us, and the *icc* cluster was therefore used to study the functions and products of the conserved five-gene cassette.

We heterologously expressed the five *icc* genes in *Aspergillus nidulans* A1145 followed by metabolite isolation and structural characterization. Co-expression of the PKS-NRPS IccA and ER IccB yielded tetramate **3** (20 mg/L) (Figure 2B, **trace ii**) (Table S4, Figures S16–20). Further coexpression of ring-expansion P450 IccC led to the production of 2-pyridone **4** that contains the *trans bis*-diene chain (20 mg/L) (Figure 2B, **trace iii**) (Table S5, Figures S21–25). The two remaining enzymes, *C*-MT IccD and OYE IccE, were then expressed in *A. nidulans*. Adding IccD to the strain that produced **4** yielded a new prominent product **2** (10 mg/L)(Figure 2B, **trace iv**). Structure characterization by NMR demonstrated **2** as the *endo* IEDDA product 8-*epi*-ilicicolin H (Table S6, Figures S26–31). This result confirmed that IccD is responsible for the transformation of *bis*-diene **4** to **2**, thus suggesting IccD acts as a pericyclase for this IEDDA reaction. After identifying **2,** we found trace amounts of **2** can be detected in IccA-C expression strain (Figure 2B, **trace iii**). Finally, adding IccE led to near complete conversion of **2** to the final product **1** (10 mg/L)(Figure 2B, **trace v**, Table S7, Figure S32–37). This assigns the role of IccE in the epimerization of **2** to **1**. The gene-by-gene reconstitution in *A. nidulans* therefore confirmed i) the five conserved enzymes IccA-IccE are necessary and sufficient to biosynthesize **1**; ii) the acyclic *bis*-diene is relatively unreactive under culturing conditions, and enzymatic acceleration of the IEDDA reaction is required; and iii) the *C*-MT homolog, IccD, catalyzes the IEDDA cycloaddition.

We then assayed the activities of IccD using *C*-His-tagged enzyme heterologously expressed and purified from *E. coli* BL21(DE3) (Figure S3). When 0.1 mM **4** was incubated with 1 μM IccD in Tris-HCl (pH 7.0), more than 60% of **4** was converted to **2** within 2 hr (Figure 3A), after which IccD denatured rapidly. The catalytic efficiency of IccD was determined by assaying the initial velocity of the transformation. IccD exhibited K_M of 54 ± 0.5 μM towards **4** and k_{cat} of 54 ± 7.8 min^{-1} (Figure S4). In the absence of IccD, the uncatalyzed reaction was nearly undetectable at room temperature in aqueous solution (Figure S5). We were able to measure the rate of uncatalyzed cycloaddition in toluene (Figure S6), with a $k_{non} = 1.8 \times 10^{-4}$ min^{-1}. Therefore, IccD is able to significantly accelerate the reaction rate by 3×10^5 fold (compared with nonenzymatic reaction measured in toluene). IccD belongs to the *C*-MT superfamily, with an intact *S*-adenosyl-L-methionine (SAM) binding motif GXGXG.[18] IccD shows 24 % homology to SpnF, also a predicted *C*-MT that catalyzes the [4+2] NEDDA cycloaddition in the biosynthesis of spinosyn.[19] Unlike the recently characterized SAM-dependent *O*-MT-like pericyclase LepI,[20] IccD did not copurify with SAM bound in the active site (Figure S7). Addition of exogenous SAM to the reaction of **4** to **2** had no effect on the reaction kinetics or product profile (Figure S8). Therefore, the IccD-catalyzed IEDDA reaction is most likely SAM-independent.

To investigate the periselectivity of IccD, we quantified product distribution resulting from IEDDA versus NEDDA reactions with and without IccD. Consistent with synthetic studies with model substrate (Figure 1B), the reaction of **4** in toluene gave **2** and **5** in a ratio of 3:1 (Figure 3B). The minor product **5** was characterized as the NEDDA product ilicicolin I (**5**) (Table S8, Figure S9 and S38–39).[11c] The reaction with IccD yielded <1% **5** (Figure 3A,B). **5** can also be detected in trace amounts from *in vivo* reconstitution using extracted ion chromatogram. This raised the possibility that **5** might be an intermediate in the IccD-catalyzed reaction of **4** to **2**. Since **5** and **2** are derived from the same facial- and *endo*-

NEDDA and IEDDA reactions, respectively, conversion of **5** to **2** could be envisioned via a [3,3]-sigmatropic Cope rearrangement (Figure 3C). However, when **5** was directly added to IccD in the reaction buffer, no **2** was formed (Figure S10). Heating **5** in water at 100°C also did not form **2 (**Figure S9). Therefore, we concluded that **5** is not an intermediate. In turn, our data point to IccD catalyzing a direct IEDDA reaction of **4** to **2** with high periselectivity.

To understand the origin of periselectivity and the potential mode of catalysis for IccD-catalyzed reaction, we performed density functional theory (DFT) calculations at the ωB97X-D/6-311+G(d,p)/CPCM(H_2O)//ωB97X-D/6-31G(d)/SMD(H_2O) and ωB97X-D/6-311+G(d,p)//ωB97X-D/6-31G(d) levels of theory.[21–24] We calculated the energy surface from **4** to **2** in the gas phase to model the hydrophobic enzyme pocket (Figure 3C). The lowest energy transition state is the ambimodal **TS-1 (**$\Delta G^{\ddagger}$=23.3 kcal·mol^{-1}) (Figure S11). Ambimodal transition states sequentially connect to a second transition state lower in energy that interconverts two products.[25] This allows **TS-1** to form both IEDDA-adduct **2** (forming C11–C16 and C8–C17) and NEDDA-adduct **5** (forming C11–C16 and C10–C19, Figure 3C) via post-transition state bifurcation. The possible Cope-rearrangement **TS-2 (**$\Delta G^{\ddagger}$=18.1 kcal·mol^{-1}) is 5.2 kcal·mol^{-1} lower in energy than **TS-1** (Figure 3C). However, cycloadducts **5** and **2** are much more stable than *bis*-diene **4**. Thus, the barrier to convert **5** to **2** ($\Delta G^{\ddagger}$=44.2 kcal·mol^{-1}) is too large for the enzyme to overcome. Hence, the enzyme must control the post-**TS-1** bifurcation dynamics to achieve high IEDDA periselectivity. Since transition state theory cannot determine the kinetic product ratio, quasi-classical reaction dynamics trajectories in gas phase were initiated from **TS-1** and found to give products **2** and **5** in a ratio of 98:2, respectively (Figure 3C, Figure S12). This ratio of **2** to **5** reproduces experimental enzymatic reactions (Figure 3B). This suggests that IccD-catalyzed reaction takes place in a hydrophobic pocket to direct the near-exclusive formation of **2** by ambimodal **TS-1**.

We also characterized the OYE homolog IccE *in vitro* to verify its role in the final epimerization step. The enzyme was expressed and purified as *N*-His-tagged protein from *E. coli* BL21(DE3)(Figure S3). When **2** was incubated with IccE in Tris-HCl (pH 7.0), the epimerization from **2** to **1** occurred readily within 2 h (Figure 2D, Figure S13). Since 8-H of **1** and **2** is relatively acidic, deprotonation of 8-H would lead to epimerization. This was demonstrated by the pH-dependent nonenzymatic epimerization from **2** to **1**, in which the epimerization rate increases as the reaction pH increases (Figure S14). IccE, as with other OYE enzymes, is predicted to be a flavin-dependent enzyme. However, no clear role of the flavin is evident in the proposed epimerization mechanism. This unexpected reactivity of IccE therefore adds to a list of nonredox reactions catalyzed by predicted flavoenzymes.[26]

The IccE-catalyzed epimerization reaction is critical for the antifungal activities of **1**, as demonstrated in our assay of **1** and **2** against *Candida albicans* SC5314. The antifungal activity of **2** (MIC = 40 μg/mL) is ~100-fold less potent compared to that of **1** (MIC = 0.4 μg/mL)(Figure S15). The epimerization reaction catalyzed by IccE can be considered as an activation step in which inversion of one stereocenter in **2** led to drastically enhanced activities. The *icc* gene cluster in *P. variabile* encodes additional redox enzymes in addition to the five conserved enzymes that synthesize **1** (Table S3). In the native host, these

additional enzymes could potentially perform modifications on **1** to further enhance its activity. In summary, our efforts uncovered the concise ilicicolin H biosynthetic pathway, featured by the pericyclase IccD that catalyzes a challenging IEDDA reaction of **4** to **2**. Our findings further expand the catalytic repertoire of naturally-occurring pericyclases.

Supplementary Material

Refer to Web version on PubMed Central for supplementary material.

ACKNOWLEDGMENTS

This work was supported by the NIH R01AI141481 to YT, R01GM 124480 to KNH and NSF (CHE-1806581) to YT and KNH. The UCLA Institute of Digital Research and Education (IDRE) provided computational resources for all calculations. MO is supported by overseas postdoctoral fellowship from The Uehara Memorial Foundation, Japan. YLZ thanks the National Natural Science Foundation of China (21377085 and 31770070).

REFERENCES

(1). Nicolaou KC; Snyder SA; Montagnon T; Vassilikogiannakis G The Diels--Alder reaction in total synthesis. Angew. Chem. Int. Ed 2002, 41, 1668–1698.

(2). Oikawa H; Tokiwano T Enzymatic catalysis of the Diels-Alder reaction in the biosynthesis of natural products. Nat. Prod. Rep 2004, 21, 321–352. [PubMed: 15162222]

(3). Jamieson CS; Ohashi M; Liu F; Tang Y; Houk KN The expanding world of biosynthetic pericyclases: cooperation of experiment and theory for discovery. Nat. Prod. Rep 2018 10.1039/c8np00075a.

(4). Tian Z; Sun P; Yan Y; Wu Z; Zheng Q; Zhou S; Zhang H; Yu F; Jia X; Chen D; Mandi A; Kurtan T; Liu W an enzymatic [4+2] cyclization cascade creates the pentacyclic core of pyrroindomycins. Nat. Chem. Biol 2015, 11, 259–265. [PubMed: 25730548]

(5). Sato M; Yagishita F; Mino T; Uchiyama N; Patel A; Chooi YH Goda Y; Xu W; Noguchi H; Yamamoto T; Hotta K; Houk KN; Tang Y; Watanabe K Involvement of lipocalin-like CghA in decalin-forming stereoselective intramolecular [4+2] Cycloaddition. Chembiochem 2015 16, 2294–2298. [PubMed: 26360642]

(6). Li L; Yu P; Tang MC; Zou Y; Gao SS; Hung YS; Zhao M; Watanabe K; Houk KN; Tang Y Biochemical characterization of a eukaryotic decalin-forming Diels−Alderase. J. Am. Chem. Soc 2016, 138, 15837–15840. [PubMed: 27960349]

(7). Kato N; Nogawa T; Takita R; Kinugasa K; Kanai M; Uchiyama M; Osada H; Takahashi S Control of the Stereochemical Course of [4+2] Cycloaddition during *trans*-Decalin Formation by Fsa2-Family Enzymes. Angew. Chem. Int. Ed. Engl 2018, 57, 9754–9758. [PubMed: 29972614]

(8). Tan D; Jamieson CS; Ohashi M; Tang M-C; Houk KN; Tang Y Genome-mined Diels-Alderase catalyzes formation of the cis-octahydrodecalins of varicidin A and B. J. Am. Chem. Soc 2019, 141, 769–773. [PubMed: 30609896]

(9). Minami A; Oikawa H Recent advances of Diels-Alderases involved in natural product biosynthesis. J Antibiot (Tokyo) 2016, 69, 500–506. [PubMed: 27301662]

(10). (a)Hayakawa S; Minato H; Katagiri K Ilicicolins, antibiotics from Cylindrocladium ilicicola. J. Antibiot 1971, 24, 653–654. [PubMed: 5167226] (b)Matsumoto M; Minato H Structure of ilicicolin H, an antifungal antibiotic. Tetrahedron. Lett 1976, 42, 3827–3830.

(11). (a)Junker B; Zhang J; Reddy MJ; Greasham G Scale-up studies on a defined medium process for pilot plant production of illicicolin by Gliocladium roseum. Biotechnol. Prog 2001, 17, 278–286. [PubMed: 11312705] (b)Liu XY; Chen XC; Qian F; Zhu T-T,; Xu JW; Li YM; Zhang LQ; Jiao BH Chlorinated phenolic sesquiterpenoids from the Arctic fungus Nectria sp. B-13. Biochem. Syst. and Ecol 2015, 59, 22–25.(c)Kildgaard S; Subko K; Phillips E; Goidts V; de la Cruz M; Diaz C; Gotfredsen CH; Andersen B; Frisvad JC; Nielsen KF; Larsen TO A dereplication and bioguided discovery dpproach to reveal new compounds from a marine-derived fungus Stilbella fimetaria. Mar. Drugs 2017, 15, E253. [PubMed: 28805711]

(12). (a)Singh SB; Liu W; Li X; Chen T; Shafiee A; Card D; Abruzzo G; Flattery A; Gill C; Thompson JR; Rosenbach M; Dreikorn S; Hornak V; Meinz M; Kurtz M; Kelly R; Onishi JC Antifungal spectrum, In vivo efficacy, and structure−activity relationship of Ilicicolin H. ACS Med. Chem. Lett 2012, 3, 814–817. [PubMed: 24900384] (b)Singh SB; Liu W; Li X; Chen T; Shafiee A; Dreikorn S; Hornak V; Meinz M; Onishi JC Structure–activity relationship of cytochrome bc1 reductase inhibitor broad spectrum antifungal ilicicolin H. Bioorg. Med. Chem. Lett 2013, 23, 3018–3022. [PubMed: 23562597]

(13). Williams DR; Bremmer ML; Brown DL; D'Antuono J Total synthesis of (±)-ilicicolin H. J. Org. Chem 1985, 50, 2807–2089.

(14). Williams DR,; Gaston RD; Horton IB Intermolecular Diels-Alder cycloaddition of bis-diene substrates. Tetrahedron. Lett 1985, 26, 1391–1394.

(15). Mukherjee D; Watts C,R; Houk KN Periselectivity in the [4 + 2] and [6 + 4] cycloadditions of diphenylnitrilimine to tropone. J. Org. Chem 1978, 43, 817–821.

(16). Halo LM; Heneghan H; Yakasai AA; Song ZS; Williams K; Bailey AM; Cox RJ Lazarus CM; Simpson TJ Late stage oxidations during the biosynthesis of the 2-pyridone tenellin in the entomopathogenic fungus Beauveria bassiana. J. Am. Chem. Soc 2008, 130, 17988–17996. [PubMed: 19067514]

(17). He XQ; Zhang ZZ,; Chen YH,; Che Q; Zhu TJ; Gu QQ; Li DH Varitatin A, a highly modified fatty acid amide from Penicillium variabile cultured with a DNA methyltransferase inhibitor. J. Nat. Prod 2015, 78, 2841–2845. [PubMed: 26561719]

(18). Schubert HL; Blumenthal RM; Cheng X Many paths to methyltransfer: a chronicle of convergence. Trends. Biochem Sci 2003, 28, 329–335. [PubMed: 12826405]

(19). Kim HJ; Ruszczycky MW; Choi SH; Liu YN; Liu HW Enzyme-catalysed [4+2] cycloaddition is a key step in the biosynthesis of spinosyn A. Nature 2011, 473, 109–112. [PubMed: 21544146]

(20). Ohashi M; Liu F; Hai Y; Chen M; Tang MC; Yang Z; Sato M; Watanabe K; Houk KN; Tang Y SAM-dependent enzyme-catalysed pericyclic reactions in natural product biosynthesis. Nature 2017, 549, 502–506. [PubMed: 28902839]

(21). Frisch MJ; Trucks GW; Schlegel HB; Scuseria GE; Robb MA; Cheeseman JR; Scalmani G; Barone V; Mennucci B; Petersson GA; Nakatsuji H; Caricato M; Li X; Hratchian HP; Izmaylov AF; Bloino J; Zheng G; Sonnenberg JL; Hada M; Ehara M; Toyota K; Fukuda R; Hasegawa J; Ishida M; Nakajima T; Honda Y; Kitao O; Nakai H; Vreven T; Montgomery JA Jr.; Peralta JE; Ogliaro F; Bearpark M; Heyd JJ; Brothers E; Kudin KN; Staroverov VN; Kobayashi R; Normand J; Raghavachari K; Rendell A; Burant JC; Iyengar SS; Tomasi J; Cossi M; Rega N; Millam JM; Klene M; Knox JE; Cross JB; Bakken V; Adamo C; Jaramillo J; Gomperts R; Stratmann RE; Yazyev O; Austin AJ; Cammi R; Pomelli C; Ochterski JW; Martin RL; Morokuma K; Zakrzewski VG; Voth GA; Salvador P; Dannenberg JJ; Dapprich S; Daniels AD; Farkas O; Foresman JB; Ortiz JV; Cioslowski J; Fox DJ Gaussian 09 Gaussian, Inc.: Wallingford, CT 2013.

(22). Chai J-D; Head-Gordon M Long-range corrected hybrid density functionals with damped atom–atom aispersion corrections. Phys. Chem. Chem. Phys 2008, 10, 6615–6620. [PubMed: 18989472]

(23). Cossi M; Rega N; Scalmani G; Barone V Energies, structures, and electronic properties of molecules in solution with the C-PCM Solvation Model. J. Comput. Chem 2003, 24, 669–681. [PubMed: 12666158]

(24). Marenich AV; Cramer CJ; Truhlar DG Universal solvation model based on solute electron density and on a continuum model of the solvent defined by the bulk dielectric constant and atomic surface tensions. J. Phys. Chem. B 2009, 113, 6378–6396. [PubMed: 19366259]

(25). (a)Caramella P; Quadrelli P; Toma LAn unexpected bispericyclic tra4sition structure leading to 4+2 and 2+4 cycloadducts in the endodimerization of cyclopentadiene. J. Am. Chem. Soc 2002, 124, 1130–1131 [PubMed: 11841256] (b)Ess DH; Wheeler SE; Iafe RG; Xu L; Celebi-Olcum N; Houk KN Bifurcations on Potential Energy Surfaces of Organic Reactions. Angew. Chem. Int. Ed 2008, 47, 7592–7601.(c)Hare SR; Tantillo DJ transition state bifurcations gain momentum - Current state of the field. Pure Appl. Chem 2017, 89, 679–698.

(26). Guarneri A; van Berkel WJ; Paul CE Alternative coenzymes for biocatalysis. Curr. Opin. Biotechnol 2019, 60, 63–71. [PubMed: 30711813]

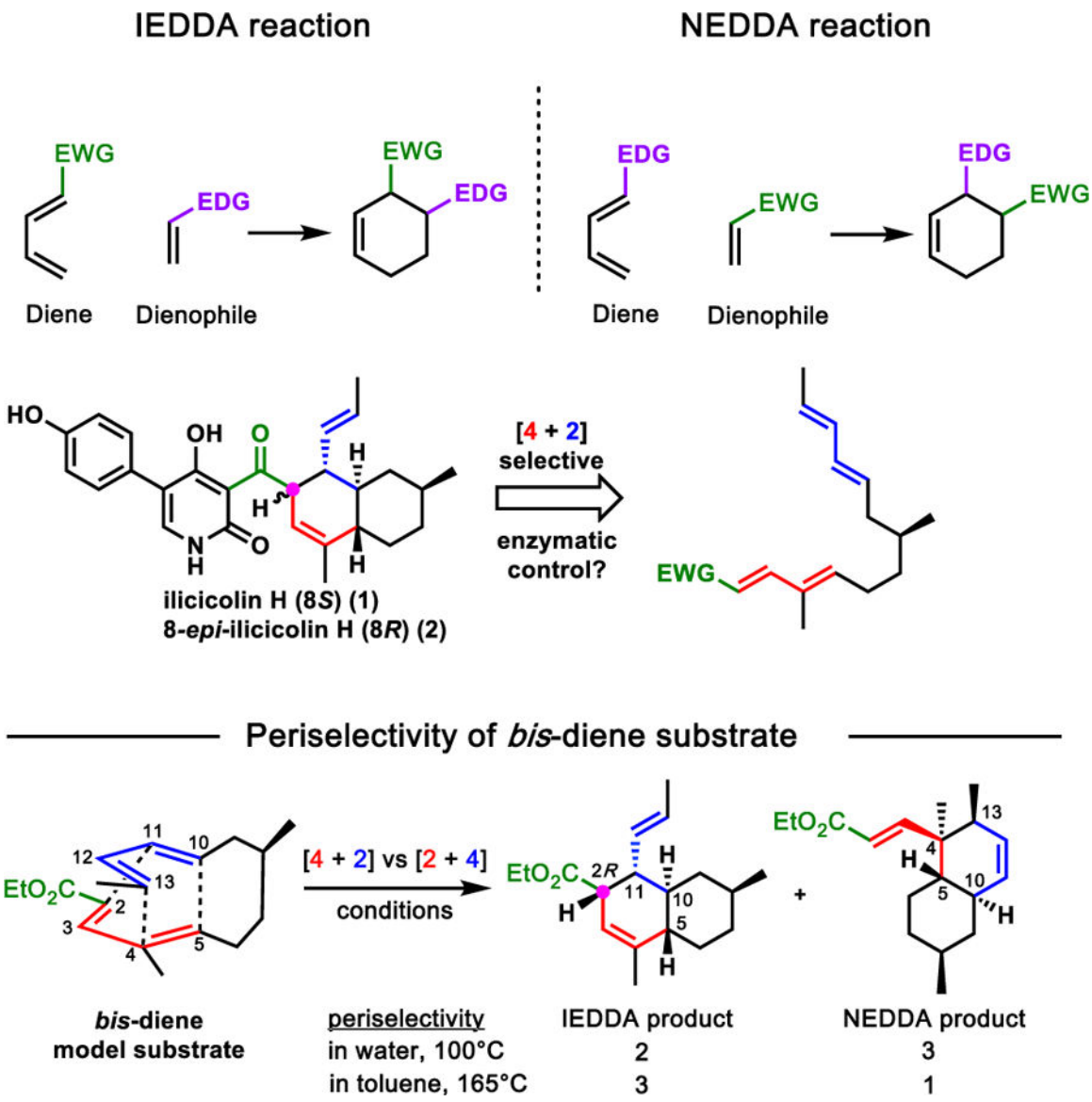

Figure 1.

NEDDA and IEDDA reactions. (**A**) General scheme of both reactions. EWG: electron withdrawing group; EDG: electron donating group; (**B**) Proposed enzyme-catalyzed IEDDA reaction in ilicicolin H (**1**) biosynthesis, as demonstrated in total synthetic effort towards **1**.

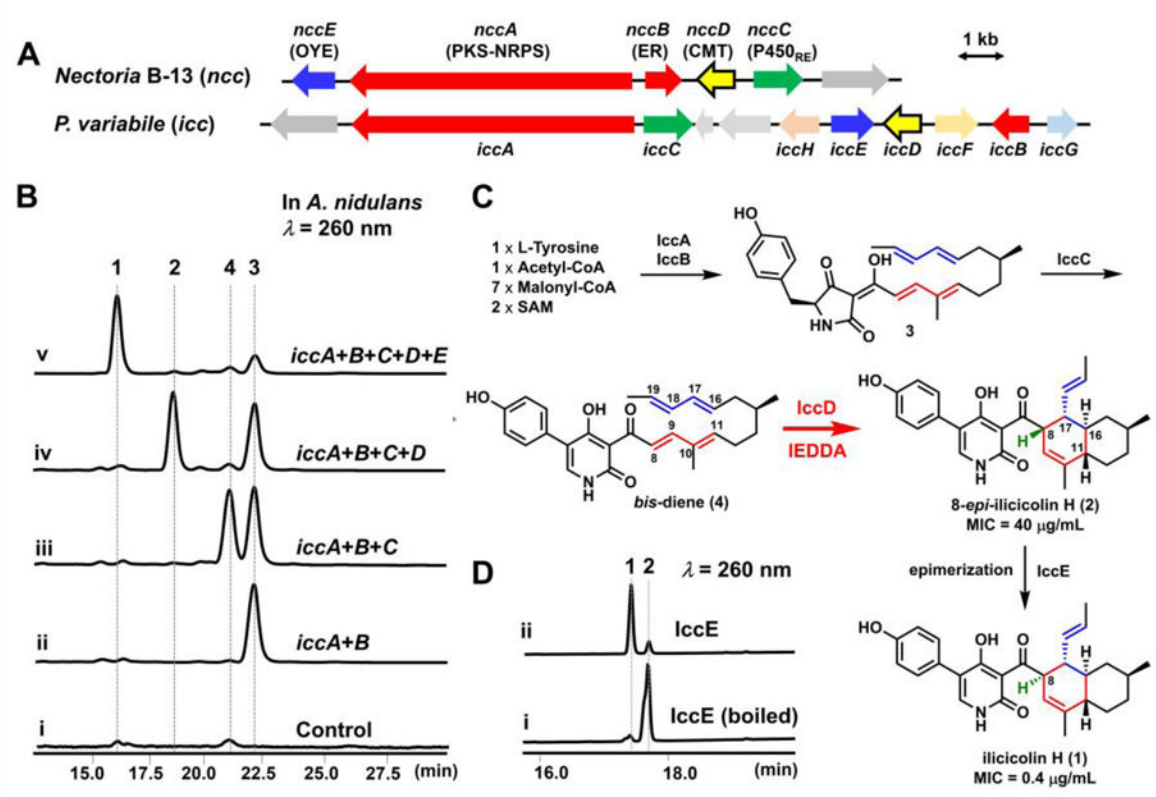

Figure 2.

Characterization of ilicicolin H (**1**) biosynthesis. **A**) The *icc* cluster encodes a PKS-NRPS (KS-AT-DH-MT-KR-ER^{o}-ACP-C-A-T-R. KS, ketosynthase; AT, acyltransferase; DH, dehydratase; MT, methyltransferase; KR, ketoreductase; ACP, acyl carrier protein; C, condensation; A, adenylation; PCP, peptidyl carrier protein; R, reductase) IccA, a *trans*-ER IccB, a ring expansion P450 IccC, a putative *C*-methyltransferase IccD and a putative old yellow enzyme IccE; **B**) Product profiles from heterologous expression of different combinations of *icc* cluster in *A. nidulans* A1145. Control in trace i is *A. nidulans* transformed with empty vectors only; **C**) Proposed biosynthetic pathway of **1**; **D**) *In vitro* characterization of IccE-catalyzed epimerization. The assays were conducted in 50 mM Tris-HCl at pH 7.0, in the presence of 0.2 mM **2** and 0.1 μM IccE.

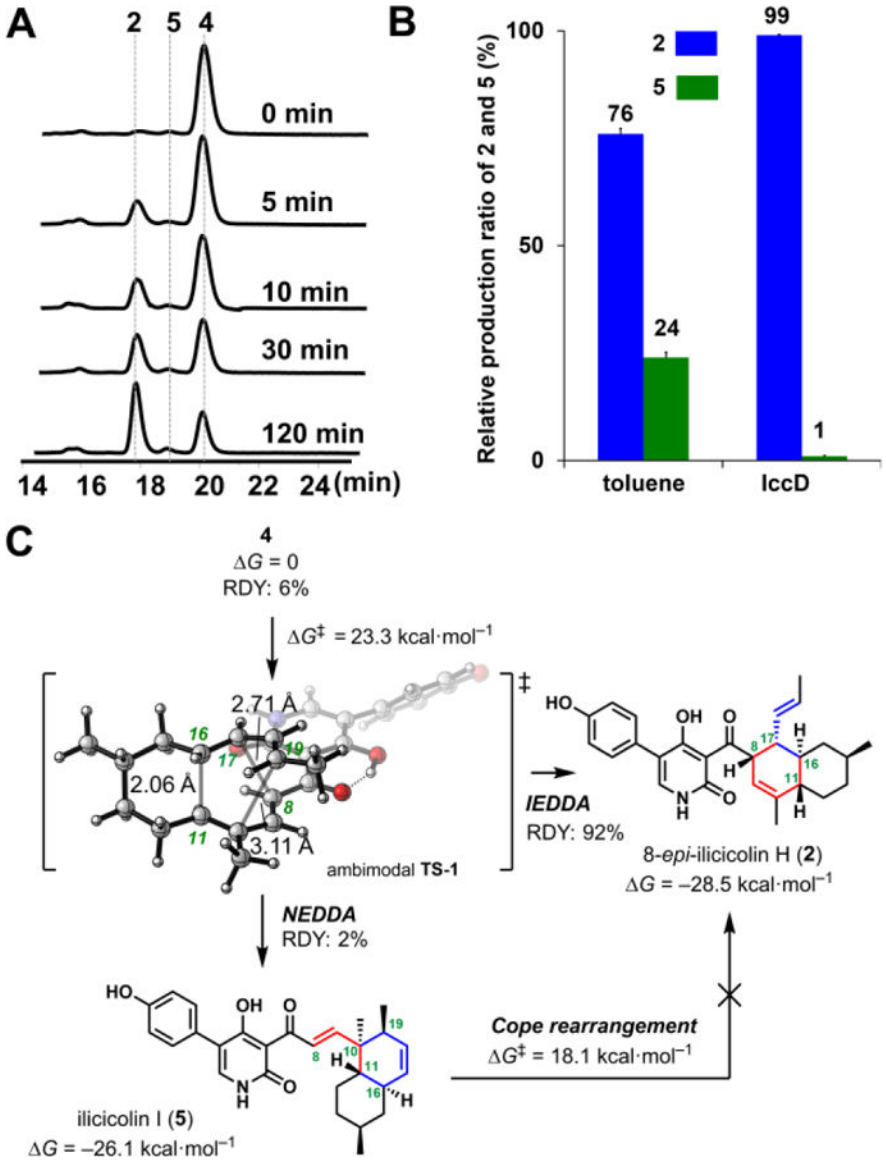

Figure 3.

Characterization of IccD-catalyzed pericyclic reaction. (**A**) HPLC profile of time-course reaction of IccD. The assays were conducted at 28°C from 0 to 120 min; (**B**) Comparison of relative IEDDA and NEDDA product ratio starting from **4**; (**C**) Calculated reaction surface energies and dynamics results from **4** converting to **2** and **5**. RDY: reaction dynamics yield from **TS-1**.